Universität Stuttgart

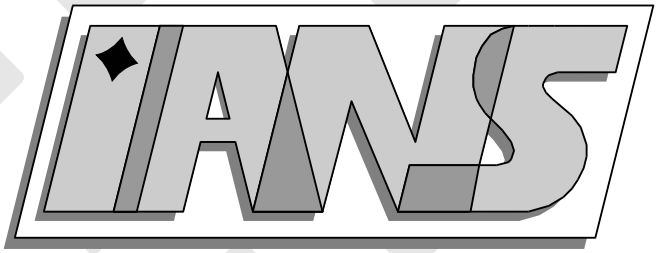

Modeling and simulation of elastoplastic forming processes

S.Brunssen

Berichte aus dem Institut für Angewandte Analysis und Numerische Simulation

Report 2006/014

Universität Stuttgart

Modeling and simulation of elastoplastic forming processes

S.Brunssen

Berichte aus dem Institut für Angewandte Analysis und Numerische Simulation

Report 2006/014

Institut für Angewandte Analysis und Numerische Simulation (IANS)
Fakultät Mathematik und Physik
Fachbereich Mathematik
Pfaffenwaldring 57
D-70 569 Stuttgart

E-Mail: ians-preprints@mathematik.uni-stuttgart.de
WWW: http://preprints.ians.uni-stuttgart.de

ISSN **1611-4176**

Modeling and simulation of elastoplastic forming processes

S. BRUNSSEN

Abstract

In order to extend the usability of implicit FE codes for large scale incremental metal forming simulations, the computation time has to be decreased dramatically. The simulation of incremental forming steps makes great demands on the elastoplastic simulation because of the permanently changing loading situation. This report gives a review over some basic concepts of metal plasticity and the need for consistent linearization of the constitutive relations.

1 Introduction

In many large scale forming simulation FE packages there is the problem that the modeling of elastoplasticity is only validated well with examples like deep-drawing or other examples, where the plastic strain, here in this work taken as the driving variable, is growing in every time step and not decreasing. A rather new class of forming operations, the so called incremental forming operations, make greater demands on the elastoplastic simulation because of the permanently changing loading situation. Especially the simulation of springback is a challenging task. In this work, much emphasize is put on the linearization of the constitutive equations and not on large deformations. In Section 2, a simple element test is introduced. A commercial FE-package (which shall be left unstated here, let us call it TEST) is compared with ABAQUS. In Section 3, we go into the details about a simple plasticity model and discuss the tangent cutting plane algorithm which is implemented in TEST. In Section 4, a classical return mapping algorithm is discussed and the so called consistently linearized material tangent is derived. In Section 5 numerical results are given.

2 Element test

A simple element test is introduced, to check, whether abrupt unloading is possible without problems or not. We compare TEST with ABAQUS [1].

Geometry One hexahedral volume element with left lower node in $[0, 0, 0]$ and right upper node in $[1, 1, 1]$ is slowly plastically loaded and abruptly elastically unloaded. Two experiments are made: One with slow plastic loading within 10 load steps and one with even slower plastic loading within 20 load steps.

In pseudo-code:

```
NODECOORDINATES
       NODE  X  Y  Z
       1     0  0  0
       2     1  0  0
       3     1  1  0
       4     0  1  0
       5     0  0  1
       6     1  0  1
       7     1  1  1
       8     0  1  1
ELEMENT TOPOLOGY
      EL.NUMBER   NODE INDICES
       1          1   2   3   4   5   6  7   8
```

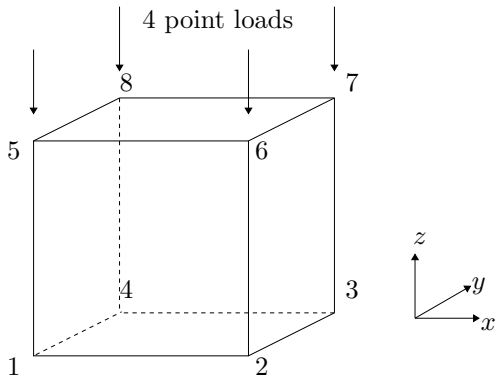

Boundary conditions

```
BOUNDARY CONDITIONS

      NODE     FIXED DOF (1 = X, 2 = Y, 3 = Z)
       1        1
       1        2
       1        3
       2        2
       2        3
       3        3
       4        1
       4        3
       5        1
       5        2
       6        2
       8        1
```

So the $z = 0$-plane fixed in z-direction, the $y = 0$-plane is fixed in y-direction and the $x = 0$-plane in x -direction.

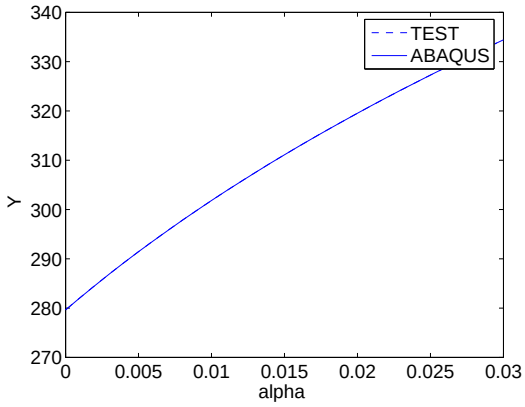

Figure 1: Nonlinear hardening curve for aluminum, in TEST given analytically and in ABAQUS given as very good approximating look-up-table

Material, yield function

$$\begin{aligned} E &= 69000 \\ \nu &= 0.33 \\ Y(\alpha) &= 646 \cdot (0.025+\alpha)^{0.227}, \quad \text{see Figure 1} \end{aligned}$$

where α denotes the equivalent plastic strain, which goes into the yield condition

$$f(\boldsymbol{\sigma}, \alpha) = \bar{\sigma}(\boldsymbol{\sigma}) - Y(\alpha) \overset{!}{\leqslant} 0.$$

Loading history

```
NODAL FORCES
   NODE    DOF    LOAD
      5     3    -69.9045
      6     3    -69.9045
      7     3    -69.9045
      8     3    -69.9045
```

This simulates a surface load of magnitude $f = 4 \cdot (-69.9045) = -Y(0)$ acting in z-direction. This surface load is multiplied with a certain factor, such that in load step the force

$$\begin{aligned} f_n &= (1+(n-1)p)f, \quad n < N \\ f_n &= 0.05f, \quad n = N \end{aligned}$$

is acting. Here, $N \in \{10, 20\}$ denotes the number of load steps and $p \in \{0.02, 0.01\}$ denotes the slope of the loading curve. What can be expected is that the first and the last load step will be elastic in both experiments. After the first step the yield surface is reached and then the nonlinear load-displacement curve is traced by load increments of 2 resp. 1 percent. In the last step the load abruptly decreases to 5 percent of the initial value to simulate elastic springback.

Results with `TEST`

The results are given in the following tables. `EPS` is the tolerance of the Newton-Raphson.

Computation with TEST, load increment 2 %

$p = 0.02$	`EPS` $=10^{-4}$		
load step	σ_{zz}	f_n	α
1	−278.87	279.62	0
2	−283.94	285.21	0.0017466
3	−288.88	290.80	0.0038576
4	−293.76	296.40	0.0060709
5	−298.59	301.99	0.008386
6	−303.37	307.58	0.010803
7	−308.09	313.17	0.013323
8	−312.75	318.76	0.015943
9	−317.35	324.36	0.018664
10	7931.4	13.98	0.26051

In step 10 no convergence is reached. The second column is not equal to the fourth column, since σ_{zz} is a Cauchy stress and therefor related to the area in the actual configuration, which is larger than in the reference configuration.

Computation with TEST, load increment 1 %

$p = 0.01$	EPS $=10^{-4}$		
load step	σ_{zz}	f_n	α
1	−278.87	279.618	0
2	−281.45	282.41418	0.00072908
3	−283.94	285.21036	0.0017467
4	−286.41	288.00654	0.0027896
5	−288.88	290.80272	0.0038579
6	−291.33	293.5989	0.0049517
7	−293.76	296.39508	0.0060712
8	−296.19	299.19126	0.0072162
9	−298.6	301.98744	0.0083867
10	−300.99	304.78362	0.0095827
11	−303.37	307.5798	0.010804
12	−305.74	310.37598	0.012051
13	−308.09	313.17216	0.013324
14	−310.43	315.96834	0.014622
15	−312.75	318.76452	0.015945
16	−315.06	321.5607	0.017293
17	−317.36	324.35688	0.018666
18	−319.63	327.15306	0.020064
19	−321.9	329.94924	0.021487
20	−13.682	13.9809	0.021487

Here step 20 converges, however 4 Newton-Raphson iterations are needed in spite of the material linearity.

Results with ABAQUS

$p = 0.02$	EPS $=10^{-4}$	
load step	α	σ_{zz}
1.	0.	−278.881
2.	$1.75027E-03$	−283.94
3.	$3.86254E-03$	−288.884
4.	$6.07672E-03$	−293.774
5.	$8.3962E-03$	−298.609
6.	$10.8155E-03$	−303.391
7.	$13.3385E-03$	−308.115
8.	$15.9616E-03$	−312.782
9.	$18.6883E-03$	−317.389
10.	$18.6883E-03$	−13.7206

Having a look into the ABAQUS message file reveals:

- no convergence problems
- no CUTBACKS
- no SEVERE DISCONTINUITY ITERATIONS
- step 1 and 10 converge within one iteration

3 Some remarks about plasticity and the Cutting Plane algorithm

3.1 Governing equations and notations

It is assumed here for simplicity that an additive decomposition of the strain tensor $\boldsymbol{\varepsilon}$ into an elastic part $\boldsymbol{\varepsilon}^e$ and a plastic part $\boldsymbol{\varepsilon}^p$ is valid. This paper is restricted to the case of isotropic hardening and to the geometric nonlinear situation. Then the general situation in associative plasticity with isotropic hardening is the following:

$$\begin{aligned} \boldsymbol{\varepsilon}^e &:= \boldsymbol{\varepsilon} - \boldsymbol{\varepsilon}^p && (1)\\ \boldsymbol{\sigma} &= \mathbf{C}^{el}\boldsymbol{\varepsilon}^e && (2)\\ \dot{\boldsymbol{\varepsilon}}^p &= \lambda \partial_{\boldsymbol{\sigma}} f(\boldsymbol{\sigma}, \alpha) && (3)\\ \dot{\alpha} &= \lambda && (4)\\ \lambda \geq 0, f(\boldsymbol{\sigma}, \alpha) \leq 0 &\quad \text{and} \quad \lambda f(\boldsymbol{\sigma}, \alpha) = 0 \end{aligned}$$

with $\boldsymbol{\sigma} \in \mathbb{S}^{3\times 3}$ the actual Cauchy stress, $\mathbb{S}^{3\times 3}$ the space of symmetric, real valued (3×3) matrices, $\lambda \in \mathbb{R}$ the plastic consistency parameter, $f : \mathbb{S}^{3\times 3} \times \mathbb{R} \to \mathbb{R}$ the yield function and the 4th order tensor $\mathbf{C}^{el}$ the elastic tangent module. The plastic anisotropy is given by the shape of the yield function f ($Y : \mathbb{R} \to \mathbb{R}$ is the function of isotropic hardening with the argument α the equivalent plastic strain):

$$f(\boldsymbol{\sigma}, \alpha) = \bar{\sigma} - Y(\alpha) \tag{5}$$

or to be more precise: it is given by the shape of the equivalent stress function

$$\bar{(\cdot)} : \mathbb{S}^{3\times 3} \to \mathbb{R}.$$

This shape can be given for example by experimentally determined R-values, see [2], p.47 and the references therein. This general situation is very difficult:

- Arbitrarily shaped yield surface (maybe even nonsmooth or nonconvex). Plastic state variables (e.g. plastic strain) **depend on** yield surface (and on the solution of course)
- And vice versa the yield surface **depends on** the plastic state variables.

So one has to deal with two nonlinearities:

1. **Global nonlinearity:** decision plastic flow or elastic behavior
2. **Element level nonlinearity:** nonlinear projection of the stress state back to the elastic region

The second nonlinearity can be reduced to a one-dimensional nonlinearity in the case of J2-plasticity (**von-Mises yield surface**).

Global equilibrium iteration

Since we assume small deformations, all integrations can be done with respect to the reference configuration Ω. By $\mathbf{V}$ we denote a suitable test space. The relation $\boldsymbol{\sigma} = \boldsymbol{\sigma}(\boldsymbol{u})$ is of course nonlinear and even not differentiable in the strong sense. The suitable notion of differentiability in the weak sense is given in the literature, see for example [6] and the references therein. A closed form of the relation is not needed here, but careful case differentiation in every load step finally results in the formula (23). A time step $t_n \to t_{n+1}$ is considered. Strong emphasis should be placed on the fact, that the stress $\boldsymbol{\sigma}_n$ does not only depend on the actual displacements $\boldsymbol{u}_n$ but also on the complete path. So there is also a dependence on $\boldsymbol{u}_{n-1}, \boldsymbol{u}_{n-2}, \ldots, \boldsymbol{u}_1$. We consider

the time step $t_n \to t_{n+1}$ and write down the global equilibrium at the actual time step t_{n+1} with the external forces $\boldsymbol{f}_{n+1}^{ext}$ acting on the body. As usual, the Cauchy stresses and the linear strain tensor are denoted by $\boldsymbol{\sigma} = \begin{bmatrix} \sigma_{xx} & \sigma_{xy} & \sigma_{xz} \\ \sigma_{yx} & \sigma_{yy} & \sigma_{yz} \\ \sigma_{zx} & \sigma_{zy} & \sigma_{zz} \end{bmatrix}$ and $\boldsymbol{\varepsilon}$. The global equilibrium equation reads like this:

$$\int_\Omega \boldsymbol{\sigma}_{n+1}(\boldsymbol{u}_{n+1}) : \boldsymbol{\varepsilon}(\boldsymbol{v}) = \int_\Omega \boldsymbol{f}_{n+1}^{ext}\ \boldsymbol{v}, \quad \boldsymbol{v} \in \mathbf{V} \tag{6}$$

The stresses are split up in old stresses and stress increments:

$$\Delta\boldsymbol{\sigma}_{n+1}(\boldsymbol{u}_{n+1}) := \boldsymbol{\sigma}_{n+1}(\boldsymbol{u}_{n+1}) - \boldsymbol{\sigma}_n(\boldsymbol{u}_n) \tag{7}$$

Then one gets:

$$\int_\Omega \Delta\boldsymbol{\sigma}_{n+1}(\boldsymbol{u}_{n+1}) : \boldsymbol{\varepsilon}(\boldsymbol{v}) = \int_\Omega \boldsymbol{f}_{n+1}^{ext}\ \boldsymbol{v} - \int_\Omega \boldsymbol{\sigma}_n(\boldsymbol{u}_n) : \boldsymbol{\varepsilon}(\boldsymbol{v}), \quad \boldsymbol{v} \in \mathbf{V} \tag{8}$$

Finite element discretization: We discretize $\boldsymbol{u}_{n+1}$ by $\boldsymbol{u}_{n+1}^h = \sum_{i=1}^N \boldsymbol{W}_i \phi_i$, $\boldsymbol{W}_i = \{U_i^x, U_i^y, U_i^z\}, \boldsymbol{U}_{n+1} = \{\boldsymbol{W}_1, \ldots, \boldsymbol{W}_N\}$ and define $\boldsymbol{F}^{int,\Delta}, \boldsymbol{F}^{ext}, \boldsymbol{F}^{int,t_0\to t_n}, \boldsymbol{F}$ in this way:

$$\begin{aligned}
F_i^{int,\Delta}(\boldsymbol{U}_{n+1}) &:= \int_\Omega \Delta\boldsymbol{\sigma}_{n+1}(\boldsymbol{U}_{n+1}) : \boldsymbol{\varepsilon}(\phi_i) && (9)\\
F_i^{ext} &= \int_\Omega \boldsymbol{f}_{n+1}^{ext}\ \phi_i && (10)\\
F_i^{int,t_0\to t_n} &:= \int_\Omega \boldsymbol{\sigma}_n : \boldsymbol{\varepsilon}(\phi_i) && (11)\\
F_i(\boldsymbol{U}_{n+1}) &:= F_i^{int,\Delta}(\boldsymbol{U}_{n+1}) - F_i^{ext} + F_i^{int,t_0\to t_n} && (12)\\
\boldsymbol{F} &= \{F_i\}_i && (13)
\end{aligned}$$

With this, we can now formulate the equilibrium equation (8) in discrete form:

$$\boldsymbol{F}(\boldsymbol{U}_{n+1}) = \mathbf{0} \tag{14}$$

Newton-Raphson iteration for elastoplastic equilibrium time step $t_n \to t_{n+1}$: The tangential stiffness $\mathbf{K}_{n+1}^{(j)} = \{K_{ik}^{(j)}\}_{ik}$ in the jth Newton step is computed, using (7). Sometimes the relation $\boldsymbol{\sigma} = \boldsymbol{\sigma}(\boldsymbol{u})$ is not written explicitly:

$$\begin{aligned}
K_{ik}^{(j)} &:= \frac{\partial F_i(\boldsymbol{U}_{n+1}^{(j)})}{\partial U_k^{(j)}} \\
&= \frac{\partial F_i^{int,\Delta}(\boldsymbol{U}_{n+1}^{(j)})}{\partial U_k^{(j)}} \\
&= \int_\Omega \frac{\partial}{\partial U_k^{(j)}}\ \Delta\boldsymbol{\sigma}_{n+1}^{(j)} : \boldsymbol{\varepsilon}(\phi_i) \\
&= \int_\Omega \boldsymbol{\varepsilon}(\phi_k) : \mathbf{C}_{n+1}^{ep,(j)} : \boldsymbol{\varepsilon}(\phi_i) && (15)
\end{aligned}$$

In the last equality, the chain rule was used with the inner derivative $\frac{\partial}{\partial U_k}\boldsymbol{\varepsilon}(\boldsymbol{U}_{n+1}) = \boldsymbol{\varepsilon}(\phi_k)$ and the outer derivative, which shall be defined as the 4th order tensor

$$\mathbf{C}_{n+1}^{ep,(j)} := \frac{\partial \Delta\boldsymbol{\sigma}_{n+1}^{(j)}}{\partial \boldsymbol{\varepsilon}(\boldsymbol{U}_{n+1}^{(j)})} = \frac{\partial \boldsymbol{\sigma}_{n+1}^{(j)}}{\partial \boldsymbol{\varepsilon}(\boldsymbol{U}_{n+1}^{(j)})} \tag{16}$$

which is denoted by elastoplastic tangent.

Algorithm (N) for solving the nonlinear problem (14)

1. Assemble stiffness matrix and right hand side according to (15) and (9) - (13)
2. Perform a Newton step for (14) (Δ has here the meaning of a Newton increment)

$$\begin{aligned} \mathbf{K}_{n+1}^{(j-1)}\ \Delta \boldsymbol{U}_{n+1}^{(j)} &= -\boldsymbol{F}(\boldsymbol{U}_{n+1}^{(j-1)}) = \boldsymbol{F}_{n+1}^{ext} - \boldsymbol{F}^{int,t_0\to t_n} - \boldsymbol{F}^{int,\Delta}(\boldsymbol{U}_{n+1}^{(j-1)}) \\ \boldsymbol{U}_{n+1}^{(j)} &= \boldsymbol{U}_{n+1}^{(j-1)} + \Delta \boldsymbol{U}_{n+1}^{(j)} \end{aligned} \tag{17}$$

3. Map the stress state back to the yield surface and update the elastoplastic tangent module according to (16):

$$\begin{aligned} &\text{CALL } [\boldsymbol{\sigma}_{n+1}^{(j)}, \mathbf{C}_{n+1}^{ep,(j)}, \alpha_{n+1}^{(j)}, \text{ELASTIC}] \\ = &\begin{cases} \text{CUTTING\_PLANE}(\boldsymbol{\varepsilon}_{n+1}^{(j)}, \boldsymbol{\varepsilon}_n, f, \alpha_n, \boldsymbol{\sigma}_n) & \text{first option, see Section 3.2} \\ \text{RADIAL\_RETURN}(\boldsymbol{\varepsilon}_{n+1}^{(j)}, \boldsymbol{\varepsilon}_n, f, \alpha_n, \boldsymbol{\sigma}_n) & \text{second option, see Section 4} \end{cases} \end{aligned}$$

4. IF ELASTIC EXIT ELSE $j := j + 1$ AND GOTO 1.

3.2 Tangent cutting plane algorithm

The following algorithm is given in [2]. It is based on works on tangent cutting plane algorithms like for example [10, 9]. A need for tangent cutting plane algorithms is given when

1. anisotropic plasticity occurs, see Figure 2 (taken from [8], p.94 and please observe that the yield function does not only change the location und size due to kinematic und isotropic hardening but also the shape due to the anisotropy), when classical return mapping algorithms do not apply any more
2. **and** when the user cannot or is not willing to provide twice differentiable yield functions in order to make general return mapping algorithms [9], Chapter 3 applicable.

Algorithm $[\boldsymbol{\sigma}_{n+1}^{(j)}, \mathbf{C}_{n+1}^{ep,(j)}, \alpha_{n+1}^{(j)}, \text{ELASTIC}] = \text{CUTTING\_PLANE}(\boldsymbol{\varepsilon}_{n+1}^{(j-1)}, \boldsymbol{\varepsilon}_n, f, \alpha_n, \boldsymbol{\sigma}_n)$

1. Elastic trial stress
   $\boldsymbol{\sigma}_{n+1}^{(j,0)} := \boldsymbol{\sigma}_n + \mathbf{C}^{el}(\boldsymbol{\varepsilon}_{n+1}^{(j-1)} - \boldsymbol{\varepsilon}_n)$

2. check yield condition
   IF $\bar{\sigma}_{n+1}^{(j,0)} - Y(\alpha_n) \leqslant 0$ THEN

   $$\text{SET } (\bullet)_{n+1}^{(j)} := (\bullet)_{n+1}^{(j,0)} \text{ AND ELASTIC := YES AND EXIT}$$

   ELSE GOTO 3

3. Initialization:
   (a) $\alpha_{n+1}^{(j,0)} := \alpha_n$
   (b) $f_{n+1}^{(j,0)} := f_n$
   (c) $\mathbf{n}_{n+1}^{(0)} := \partial_{\boldsymbol{\sigma}} f|_{\boldsymbol{\sigma}_{n+1}^{(j,0)}} \in \mathbb{R}^{3\times 3}$ flow direction
   (d) $A_{n+1}^{(0)} := \partial_{\alpha} f|_{\alpha_{n+1}^{(j,0)}} + \mathbf{n}_{n+1}^{(0)} : \mathbf{C}^{el} : \mathbf{n}_{n+1}^{(0)}$
   (e) $\lambda^{(0)} := 0$
   (f) $Y_{n+1}^{(0)} := Y(\alpha_n)$

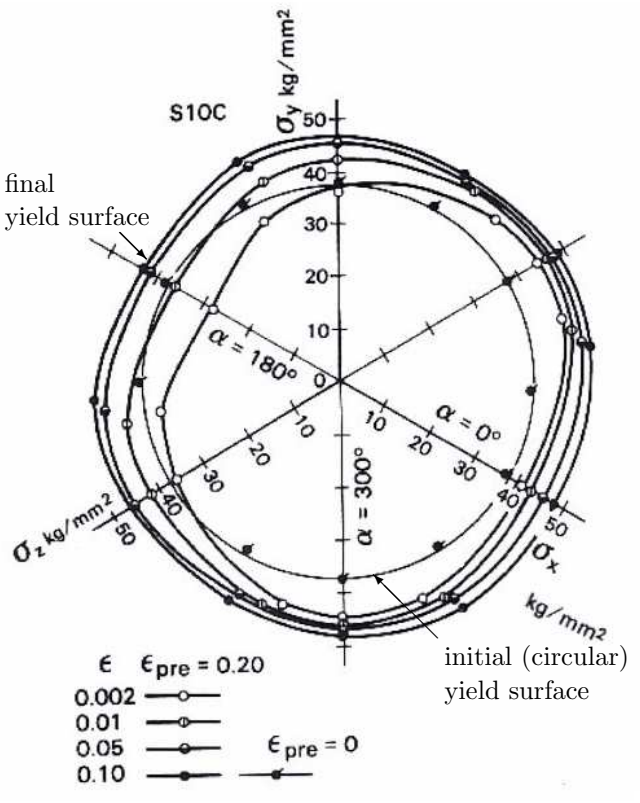

Figure 2: Anisotropic yield surface for the steel S10C, for different plastic strains, taken from [2]

4. ITERATION $i = 0, 1, 2, \ldots$
   (a) $\Delta\lambda^{(i+1)} := \frac{\bar{\sigma}^{(j,i)}_{n+1} - Y^{(i)}_{n+1}}{A^{(i)}_{n+1}}$
   (b) $\boldsymbol{\sigma}^{(j,i+1)}_{n+1} := \boldsymbol{\sigma}^{(j,i)}_{n+1} - \Delta\lambda^{(i+1)}\mathbf{C}^{el} : \mathbf{n}^{(i)}_{n+1}$
   (c) $\bar{\sigma}^{(j,i+1)}_{n+1} := \bar{\sigma}(\boldsymbol{\sigma}^{(j,i+1)}_{n+1})$
   (d) $\mathbf{n}^{(i+1)}_{n+1} := \partial_{\boldsymbol{\sigma}} f|_{\boldsymbol{\sigma}^{(j,i+1)}_{n+1}}$
   (e) $A^{(i+1)}_{n+1} := \partial_{\alpha} Y|_{\alpha^{(j,i)}_{n+1}} + \mathbf{n}^{(i+1)}_{n+1} : \mathbf{C}^{el} : \mathbf{n}^{(i+1)}_{n+1}$
   (f) $\lambda^{(i+1)} := \lambda^{(i)} + \Delta\lambda^{(i+1)}$
   (g) $\Delta\alpha^{(j,i+1)}_{n+1} := \lambda^{(i+1)}$
   (h) $\alpha^{(j,i+1)}_{n+1} := \alpha_n + \Delta\alpha^{(j,i+1)}_{n+1}$
   (i) $Y^{(i+1)}_{n+1} := Y(\alpha^{(j,i+1)}_{n+1})$
   (j) IF $\bar{\sigma}^{(i+1,j)}_{n+1} - Y^{(i+1)}_{n+1} < \varepsilon^{tol}$ THEN
   INNER ITERATION FINISHED, ELASTIC := NO, GOTO 5
   ELSE $i = i + 1$ GOTO 4
   ENDIF
5. elastoplastic module $\mathbf{C}^{ep,(j)}_{n+1} := \mathbf{C}^{el} - \frac{1}{A_{n+1}}(\mathbf{C}^{el} : \mathbf{n}_{n+1}) \otimes (\mathbf{C}^{el} : \mathbf{n}_{n+1})$

Details about the background can be found in [2]. Only a few points are discussed here, especially the elastoplastic module.

Fulfillment of the yield condition (4a,4e,4f): In [2], two different hardening theories are mentioned (W_p is the plastic dissipation):

$$\begin{aligned} f(\boldsymbol{\sigma}, W_p) &:= \bar{\sigma}(\boldsymbol{\sigma}) - Y(W_p) \quad \text{work-hardening theory} \\ f(\boldsymbol{\sigma}, \alpha) &:= \bar{\sigma}(\boldsymbol{\sigma}) - Y(\alpha) \quad \text{strain-hardening theory} \end{aligned} \tag{18}$$

Only strain-hardening is considered here. An equation for the plastic consistency parameter has to be developed, such that the yield condition is fulfilled in the actual load step respectively in the actual Newton step.

$$f_{n+1}^{(j)}(\lambda) = f(\boldsymbol{\sigma}_{n+1}^{(j)}(\lambda), \alpha_{n+1}^{(j)}(\lambda)) \stackrel{!}{=} 0 \tag{19}$$

From this follows with (5):

$$\begin{aligned} \partial_\lambda f_{n+1}^{(j)} &= \partial_{\boldsymbol{\sigma}} f_{n+1}^{(j)} : \partial_\lambda \boldsymbol{\sigma}_{n+1}^{(j)} + \partial_Y f_{n+1}^{(j)} \; \partial_\alpha Y_{n+1}^{(j)} \; \partial_\lambda \alpha_{n+1}^{(j)} \\ &= -\partial_{\boldsymbol{\sigma}} f_{n+1}^{(j)} : \mathbf{C}_{n+1}^{el} : \partial_{\boldsymbol{\sigma}} f_{n+1}^{(j)} - \partial_\alpha Y_{n+1}^{(j)} \end{aligned}$$

The last equation is obtained with the aid of

$$\begin{aligned} \boldsymbol{\varepsilon}_{n+1}^{p,(j)} - \boldsymbol{\varepsilon}_n^p &= \lambda \, \partial_{\boldsymbol{\sigma}} f_{n+1}^{(j)} \qquad \text{(implicit Euler scheme for Equation (3))} \\ \boldsymbol{\sigma}_{n+1}^{(j)} - \boldsymbol{\sigma}_n &= \mathbf{C}^{el} : [\boldsymbol{\varepsilon}_{n+1} - \boldsymbol{\varepsilon}_{n+1}^{p,(j)} - \boldsymbol{\varepsilon}_n + \boldsymbol{\varepsilon}_n^p] \\ &= \mathbf{C}^{el} : [\boldsymbol{\varepsilon}_{n+1} - \boldsymbol{\varepsilon}_n - \lambda \, \partial_{\boldsymbol{\sigma}} f_{n+1}^{(j)}] \end{aligned}$$

and 4. Note that the total strain $\boldsymbol{\varepsilon}_{n+1}$ does not depend on λ. So the Newton scheme for finding the root of f reads like this:

$$\partial_\lambda f_{n+1}^{(j)}|_{\lambda^{(i)}} \, \Delta\lambda^{(i+1)} = -f_{n+1}^{(j)}(\lambda^{(i)})$$

with

$$\Delta\lambda^{(i+1)} = \frac{f_{n+1}^{(j)}(\lambda^{(i)})}{\partial_{\boldsymbol{\sigma}} f_{n+1}^{(j)} : \mathbf{C}^{el} : \partial_{\boldsymbol{\sigma}} f_{n+1}^{(j)} + \partial_\alpha Y_{n+1}^{(j)}}$$

3.3 Discussion

One of the problems arising here, is that the yield condition is fulfilled but $\mathbf{C}_{n+1}^{ep,(j)}$ in Point 5 of Algorithm `CUTTING_PLANE` is not the consistent material tangent. Indeed one can see that (16) is not fulfilled by the tangent cutting plane algorithm presented here. In fact it is derived from the time-continuous $\mathbf{C}^{ep} = \frac{\partial \boldsymbol{\sigma}}{\partial \boldsymbol{\varepsilon}}$, see for example [2]. As it is shown in the results at the end of this work, that no good convergence is achievable, using this tangent.

4 Consistent linearization in the case of linear isotropic hardening

Now the radial return algorithm for linear isotropic hardening is described. One sees that within the framework of this stress integration algorithm, a consistent material tangent can be obtained. Except for minor technical details, the resulting algorithm is the same as documented in e.g. [9].

Governing equations The yield function is now specified to a von-Mises type of yield function with linear isotropic hardening.

$$\begin{aligned} a_0 &:= \sqrt{\frac{3}{2}} \qquad \text{auxiliary variable} \\ \tilde{\lambda} &:= a_0^2 \lambda \\ \mathbf{s} &:= \operatorname{dev}(\boldsymbol{\sigma}) \\ \bar{\sigma} &:= a_0 \sqrt{\operatorname{dev}(\boldsymbol{\sigma}) : \operatorname{dev}(\boldsymbol{\sigma})} \\ ||\boldsymbol{\sigma}|| &:= \sqrt{\boldsymbol{\sigma} : \boldsymbol{\sigma}} \\ Y(\alpha) &:= Y(0) + H\ \alpha \\ f(\boldsymbol{\sigma}, \alpha) &:= \bar{\sigma} - Y(\alpha) \end{aligned} \tag{20}$$

By $H \in \mathbb{R}_+$, the constant hardening parameter is denoted. Because of the structure of f, the ODE for the evolution of the plastic strain can be written explicitly in terms of the stress.

$$\dot{\boldsymbol{\varepsilon}}^p = \lambda \frac{a_0 \mathbf{s}}{||\mathbf{s}||} = \tilde{\lambda} \frac{\mathbf{s}}{\bar{s}} \tag{21}$$

In the following algorithm, the notation $\mathbf{1}$ and $\mathbf{I}_{dev} = \mathbf{I} - \frac{1}{3}\mathbf{1} \otimes \mathbf{1}$ are used for the second oder identity tensor and the fourth order deviatoric tensor.

Algorithm $[\boldsymbol{\sigma}_{n+1}^{(j)}, \mathbf{C}_{n+1}^{ep,(j)}, \alpha_{n+1}^{(j)}, \text{ELASTIC}] = \text{RADIAL\_RETURN}(\boldsymbol{\varepsilon}_{n+1}^{(j-1)}, \boldsymbol{\varepsilon}_n, f, \alpha_n, \boldsymbol{\sigma}_n)$

1. Compute trial elastic stress $\mathbf{s}_{n+1}^{tr}$

$$\begin{aligned} \boldsymbol{e}_{n+1} &:= \mathbf{I}_{dev} \boldsymbol{\varepsilon}_{n+1}^{(j-1)} && \text{deviatoric strain} \\ \mathbf{s}_{n+1}^{tr} &:= 2\mu(\boldsymbol{e}_{n+1} - \boldsymbol{e}_n^p) && \text{trial deviatoric stress} \\ \boldsymbol{\sigma}_{n+1}^{tr} &:= \kappa \operatorname{tr}(\boldsymbol{\varepsilon}_{n+1}^{(j-1)})\ \mathbf{1} + \mathbf{s}_{n+1}^{tr} && \text{trial stress} \end{aligned}$$

2. Check yield condition

$$f_{n+1}^{tr} := \bar{\sigma}_{n+1}^{tr} - Y(\alpha_n) \quad \text{evaluation of the yield function}$$

IF $f_{n+1}^{tr} \leqslant 0$ THEN:

$$\text{SET } (\bullet)_{n+1}^{(j)} := (\bullet)_{n+1}^{tr} \text{ AND ELASTIC := YES AND EXIT}$$

ENDIF

3. Compute flow direction $\mathbf{n}_{n+1}$ and plastic consistency parameter λ

$$\begin{aligned} \lambda &:= \text{root}[g(\lambda) = 0] && \text{plastic consistency parameter, see Section 4.1.1} \\ \mathbf{n}_{n+1} &:= \frac{1}{||\mathbf{s}_{n+1}^{tr}||} \mathbf{s}_{n+1}^{tr} && \text{flow direction} \\ \tilde{\mathbf{n}}_{n+1} &:= a_0^{-1}\ \mathbf{n}_{n+1} && \text{scaled flow direction} \\ \alpha_{n+1}^{(j)} &:= \alpha_n + a_0^{-2} \tilde{\lambda} && \text{implicit Euler for (4)} \end{aligned} \tag{22}$$

4. Update backstress, plastic strain and stress

$$\begin{aligned} \boldsymbol{e}_{n+1}^p &\overset{(21)}{:=} \boldsymbol{e}_n^p + \tilde{\lambda} \tilde{\mathbf{n}}_{n+1} && \text{plastic strain} \\ \boldsymbol{\sigma}_{n+1}^{(j)} &:= \kappa \operatorname{tr}(\boldsymbol{\varepsilon}_{n+1}^{(j-1)}) \mathbf{1} + \mathbf{s}_{n+1}^{tr} - 2\mu\tilde{\lambda}\tilde{\mathbf{n}}_{n+1} \\ &= \kappa \operatorname{tr}(\boldsymbol{\varepsilon}_{n+1}^{(j-1)}) \mathbf{1} + \mathbf{s}_{n+1}^{tr} - 2\mu a_0 \lambda \mathbf{n}_{n+1} \end{aligned} \tag{23}$$

5. Compute the *consistent* elastoplastic tangent module $\mathbf{C}^{ep}$ according to Equation (24)

4.1 Consistent elastoplastic tangent module

For the sake of brevity, the index for the Newton iteration (j) is omitted in the following. With (25) and some equations from tensor calculus, see the Appendix, the following derivatives can be computed:

$$\begin{aligned}
\partial_{\boldsymbol{\varepsilon}_{n+1}}(\mathrm{tr}(\boldsymbol{\varepsilon}_{n+1})\mathbf{1}) &= \mathbf{1}\otimes\mathbf{1} \\
\partial_{\boldsymbol{\varepsilon}_{n+1}}(\lambda\mathbf{n}_{n+1}) &= \mathbf{n}_{n+1}\otimes\frac{\partial\lambda}{\partial\boldsymbol{\varepsilon}_{n+1}} - \lambda\frac{\partial\mathbf{n}_{n+1}}{\partial\boldsymbol{\varepsilon}_{n+1}} \\
\frac{\partial\lambda}{\partial\boldsymbol{\varepsilon}_{n+1}} &= \frac{a_0^{-1}}{\frac{2}{3}H+2\mu}\frac{\mathbf{s}^{tr}_{n+1}}{||\mathbf{s}^{tr}_{n+1}||} : \frac{\partial\mathbf{s}^{tr}_{n+1}}{\partial\boldsymbol{\varepsilon}_{n+1}} = \frac{a_0^{-1}}{\frac{2}{3}H+2\mu}2\mu\frac{\mathbf{s}^{tr}_{n+1}}{||\mathbf{s}^{tr}_{n+1}||} \\
&= 2\mu\ \frac{a_0^{-1}}{\frac{2}{3}H+2\mu}\ \mathbf{n}_{n+1}
\end{aligned}$$

And moreover:

$$\begin{aligned}
\partial_{\boldsymbol{\varepsilon}n+1}\mathbf{n}_{n+1} &= \frac{\partial\mathbf{n}_{n+1}}{\partial\mathbf{s}^{tr}_{n+1}}\ \frac{\partial\mathbf{s}^{tr}_{n+1}}{\partial\boldsymbol{\varepsilon}_{n+1}} \\
&= \frac{1}{||\mathbf{s}^{tr}_{n+1}||}(\mathbf{I}-\mathbf{n}_{n+1}\otimes\mathbf{n}_{n+1})\frac{\partial\mathbf{s}^{tr}_{n+1}}{\partial\boldsymbol{\varepsilon}_{n+1}} \\
&= \frac{1}{||\mathbf{s}^{tr}_{n+1}||}(\mathbf{I}-\mathbf{n}_{n+1}\otimes\mathbf{n}_{n+1})2\mu\mathbf{I}_{dev} \\
&= \frac{2\mu}{||\mathbf{s}^{tr}_{n+1}||}(\mathbf{I}_{dev}-\mathbf{n}_{n+1}\otimes\mathbf{n}_{n+1}) \qquad (\mathbf{n}_{n+1}\text{ deviatoric})
\end{aligned}$$

With this, one arrives at the desired tangent module:

$$\begin{aligned}
\mathbf{C}^{ep} &= \frac{\partial\boldsymbol{\sigma}_{n+1}}{\partial\boldsymbol{\varepsilon}_{n+1}} \\
&= \kappa\ \mathbf{1}\otimes\mathbf{1} + 2\mu\ \mathbf{I}_{dev} - 2\mu\ a_0\left[\mathbf{n}_{n+1}\otimes\frac{\partial\lambda}{\partial\boldsymbol{\varepsilon}_{n+1}} + \lambda\frac{\partial\mathbf{n}_{n+1}}{\partial\boldsymbol{\varepsilon}_{n+1}}\right] \\
&= \mathbf{C}^{el} - 2\mu\ a_0\ \mathbf{n}_{n+1}\otimes 2\mu\ \frac{a_0^{-1}}{\frac{2}{3}H+2\mu}\ \mathbf{n}_{n+1} - 2\mu\ a_0\ \frac{2\mu\lambda}{||\mathbf{s}^{tr}_{n+1}||}(\mathbf{I}_{dev}-\mathbf{n}_{n+1}\otimes\mathbf{n}_{n+1}) \\
&= \mathbf{C}^{el} - 2\mu\frac{2\mu\ \tilde{\lambda}}{\bar{s}^{tr}_{n+1}}\ \mathbf{I}_{dev} - 2\mu\frac{3}{2}\tilde{\theta}\ \tilde{\mathbf{n}}_{n+1}\otimes\tilde{\mathbf{n}}_{n+1} \qquad (24)
\end{aligned}$$

with the abbreviation $\tilde{\theta} := \frac{2\mu}{\frac{2}{3}H+2\mu} - \frac{2\mu\ \tilde{\lambda}}{\bar{s}^{tr}_{n+1}}$.

4.1.1 Plastic consistency parameter

The aim of this section is to compute an expression for the plastic consistency parameter λ. The deviatoric part of Equation (23) is:

$$\mathbf{s}_{n+1} - \mathbf{s}^{tr}_{n+1} + 2\mu a_0\lambda\ \mathbf{n}_{n+1} = \mathbf{0}$$

Multiplying this with $\mathbf{n}^{\top}_{n+1}$ and using that

$$\mathbf{n}_{n+1} = \frac{\mathbf{s}^{tr}_{n+1}}{||\mathbf{s}^{tr}_{n+1}||} = \frac{\mathbf{s}_{n+1}}{||\mathbf{s}_{n+1}||}$$

one gets:

$$g(\lambda) := ||\mathbf{s}_{n+1}|| - ||\mathbf{s}^{tr}_{n+1}|| + 2\mu a_0\lambda = 0$$

Using that the yield condition is fulfilled at t_{n+1} and with the aid of (22), one can compute:

$$\begin{aligned} g(\lambda) &= a_0^{-1} Y(\alpha_{n+1}) - ||\mathbf{s}_{n+1}^{tr}|| + 2\mu a_0 \lambda \\ &= a_0^{-1} Y(0) + a_0^{-1} H \alpha_{n+1} - ||\mathbf{s}_{n+1}^{tr}|| + 2\mu a_0 \lambda \\ &= a_0^{-1} Y(0) + a_0^{-1} H(\alpha_n + \lambda) - ||\mathbf{s}_{n+1}^{tr}|| + 2\mu a_0 \lambda \end{aligned}$$

Finally one arrives with (20) at:

$$\lambda = \frac{\frac{2}{3}(-Y(0) - H\ \alpha_n) + a_0^{-1}||\mathbf{s}_{n+1}^{tr}||}{2\mu + \frac{2}{3}H} \tag{25}$$

$$\Leftrightarrow \quad \tilde{\lambda} = \frac{-Y(0) - H\alpha_n + \bar{s}_{n+1}^{tr}}{H + 2\mu} \tag{26}$$

5 Numerical results

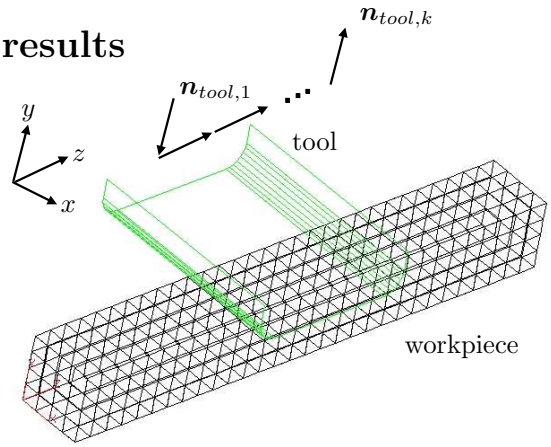

Figure 3: Problem setting of the forging simulation

In this section, the both approaches are compared, considering an elastoplastic forging like simulation, depicted in Figure 3. The assumptions are J2 plasticity and linear isotropic hardening and small deformations. So the element, which was formulated for the more general case of anisotropic plasticity is expected to behave like the revised element with the consistently formulated Radial Return algorithm. Results for ($\boldsymbol{n}_{tool,k}$ = tool feed in step k)

$$\boldsymbol{n}_{tool,1,\ldots,5} = \begin{bmatrix} 0 \\ -0.05 \\ 0 \end{bmatrix}, \boldsymbol{n}_{tool,6,\ldots,50} = \begin{bmatrix} 0 \\ 0 \\ 0.1 \end{bmatrix}$$

are given in Figure 4. To compare the convergence of the Newton scheme between Radial Return (RR) and Tangent Cutting Plane (CP) elements and to see how the behavior in the case of spring back, this slightly modified example is considered. The results are given in Figure 5.

$$\boldsymbol{n}_{tool,1,\ldots,5} = \begin{bmatrix} 0 \\ -0.05 \\ 0 \end{bmatrix}, \boldsymbol{n}_{tool,6,\ldots,20} = \begin{bmatrix} 0 \\ 0 \\ 0.1 \end{bmatrix}, \boldsymbol{n}_{tool,23} = \begin{bmatrix} 0 \\ 0.05 \\ 0 \end{bmatrix}$$

Obviously the (RR) element performs much better, especially in the springback situation. To rule out the possibility, that the (RR) performs better than (CP), because it only handles small deformations, another example with even smaller deformations is given with results in Figure 6. Although this experiment is much nearer to the geometric situation, the (CP) element does not perform much better.

$$\boldsymbol{n}_{tool,1} = \begin{bmatrix} 0 \\ -0.05 \\ 0 \end{bmatrix}, \boldsymbol{n}_{tool,2,\ldots,23} = \begin{bmatrix} 0 \\ 0 \\ 0.1 \end{bmatrix}$$

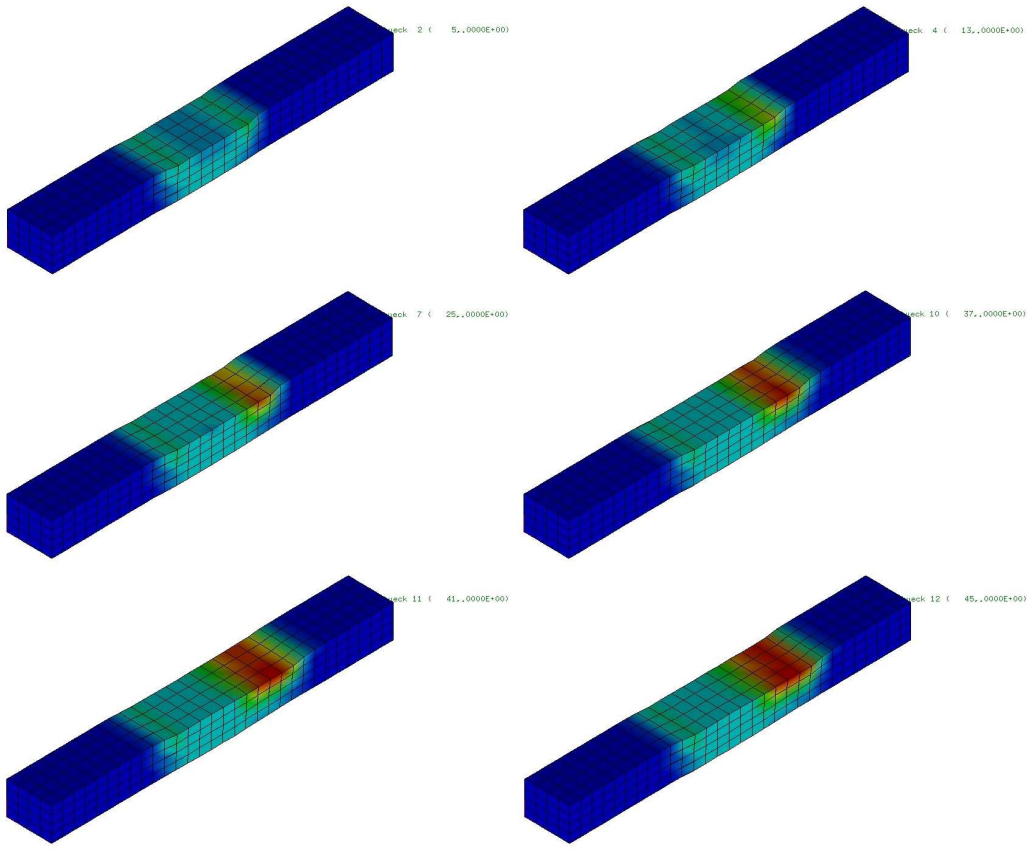

Figure 4: Steps 5,13,25,37,41 and 45 of the forging simulation, the evolution of the hardening parameter α is shown

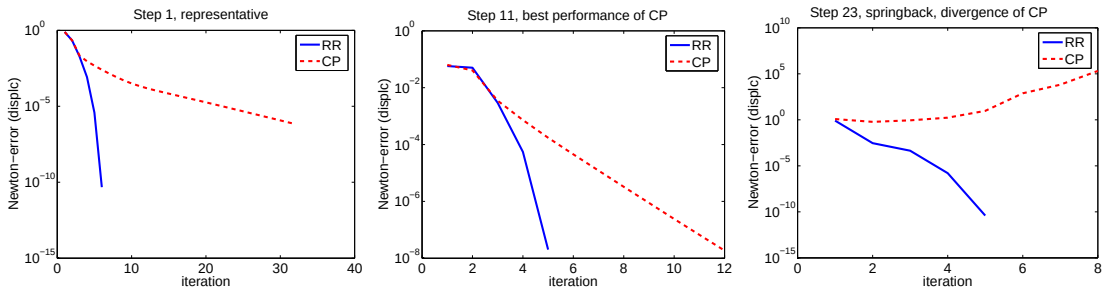

Figure 5: $\frac{||\Delta \boldsymbol{U}^{(j)}||}{||\Delta \boldsymbol{U}^{(1)}||}$ plotted over the Newton iteration (j)

Appendix

Some rules from tensor calculus are given here. Tensors of 2nd order are written in small fat letters and 4th order tensors in capital fat letters.

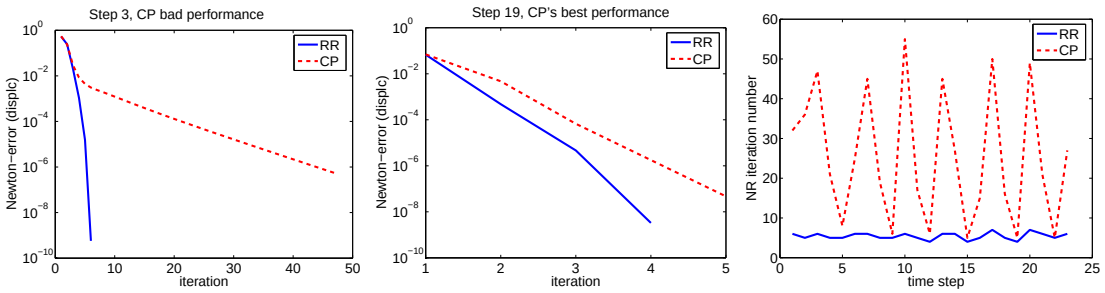

Figure 6: $\frac{||\Delta \boldsymbol{U}^{(j)}||}{||\Delta \boldsymbol{U}^{(1)}||}$ plotted over the Newton iteration (j) and comparison over the Newton iteration numbers over the whole time step

$$\mathbf{1} := \delta_{ij} \qquad \text{2nd order identity tensor}$$

$$\mathbf{I} := \frac{1}{2}(\delta_{ik}\delta_{jl} + \delta_{il}\delta_{jk}) \qquad \text{sym. 4th order identity tensor}$$

$$\mathrm{tr}(\mathbf{b}) := \mathbf{1} : \mathbf{b}$$

$$(\mathbf{b} \otimes \mathbf{c})\mathbf{d} := (\mathbf{c} : \mathbf{d})\mathbf{b} \tag{27}$$

$$\mathbf{I}_{tr} := \frac{1}{3}\mathbf{1} \otimes \mathbf{1} \qquad \text{4th order trace tensor} \tag{28}$$

$$\Rightarrow \mathbf{I}_{tr}\mathbf{b} = \frac{1}{3}\mathrm{tr}(\mathbf{b})\mathbf{1}$$

$$\mathbf{I}_{dev} := \mathbf{I} - \frac{1}{3}\mathbf{1} \otimes \mathbf{1} \qquad \text{4th order deviatoric tensor}$$

$$\partial_{\boldsymbol{\varepsilon}} \mathrm{tr}(\boldsymbol{\varepsilon}) = \mathbf{1} \tag{29}$$

$$\frac{\partial(\alpha \mathbf{S})}{\partial \mathbf{T}} = \mathbf{S} \otimes \frac{\partial \alpha}{\partial \mathbf{T}} + \alpha \frac{\partial \mathbf{S}}{\partial \mathbf{T}} \tag{30}$$

$$\boldsymbol{n}(\boldsymbol{\xi}) := \frac{\boldsymbol{\xi}}{||\boldsymbol{\xi}||}$$

$$\partial_{\boldsymbol{\varepsilon}} ||\boldsymbol{\xi}|| = \boldsymbol{n} : \partial_{\boldsymbol{\varepsilon}} \boldsymbol{\xi} \tag{31}$$

$$\Rightarrow \partial_{\boldsymbol{\xi}} \boldsymbol{n} = \frac{1}{||\boldsymbol{\xi}||}(\mathbf{I} - \boldsymbol{n} \otimes \boldsymbol{n}) \tag{32}$$

$$\mathbf{A} : \mathbf{B} := A_{ijkl}\, B_{klmn}$$

6 Summary

It was shown in this work, that the importance of correct derivatives in the material stiffness matrix cannot be overestimated in the context of metal forming. In principle similar good convergence is not only achievable in the very simple case of J2 plasticity but also in the case of a general anisotropic yield function and a nonlinear isotropic and kinematic hardening law, see [9] p. 146.

7 Ackknowledgements

The work in this paper was funded by the German Research Foundation (DFG) through the project WO671/4-1 in the framework of SPP1146: Modeling of incremental forming operations.

References

[1] Abaqus, `http://www.abaqus.com/`

[2] H. Aretz, *Modellierung des anisotropen Materialverhaltens von Blechen mit Hilfe der Finite-Elemente-Methode*, Dissertation, Fakultät für Bergbau, Hüttenwesen und Geowissenschaften, RWTH Aachen (2003)

[3] J.H. Argyris, H. P. Mlejnek, *Die Methode der Finiten Elemente, Band I*, Vieweg, 1986

[4] J.H. Argyris, H. P. Mlejnek, *Die Methode der Finiten Elemente, Band II*, Vieweg, 1987

[5] T. Belytschko and W.K. Liu and B. Moran, *Nonlinear Finite Elements for Continua and Structures*, John Wiley & Sons, 2000

[6] P.W. Christensen, *A nonsmooth Newton method for elastoplastic problems*, Computer methods in applied mechanics and engineering;**191**:1189–1219 (2002)

[7] W. Han, B.D. Reddy, *Plasticity, Mathematical Theory and Numerical Analysis*, Springer, 1999

[8] D.P. Koistinen, N.M. Wang, *Mechanics of sheet metal forming - material behavior and deformation analysis*, Plenum Press, 1978

[9] J.C. Simo, T.J.R. Hughes, *Computational Inelasticity*, Springer 1998

[10] J. C. Simo, M. Ortiz, *A unified approach to finite deformation elastoplastic analysis based on the use of hyperelastic constitutive equations*, Computer Methods in Applied Mechanics and Engineering;**49**:221–245 (1985)

Erschienene Preprints ab Nummer 2006/001

Komplette Liste: `http://preprints.ians.uni-stuttgart.de`

2006/001 *Klimke, A.:* Sparse Grid Interpolation Toolbox - User's Guide

2006/002 *Klimke, A., Wohlmuth, B.:* Constructing Dimension-Adaptive Sparse Grid Interpolants using Parallel Function Evaluations

2006/003 *Hartmann, S., Brunssen, S., Ramm, E., Wohlmuth, B.:* Application of a primal-dual active set strategy for unilateral non-linear dynamic contact problems of thin-walled structures

2006/004 *Sändig, A.-M.:* Partielle Differentialgleichungen Vorlesung im Wintersemester 2005/2006

2006/005 *Nicaise, S., Witowski, K., Wohlmuth, B.:* An a posteriori error estimator for the Lame equation based on H(div)-conforming stress approximations

2006/006 *Geis, W. (ed.), Sändig, A.-M. (ed.):* Second International Workshop - Direct and Inverse Problems in Piezoelectricity,Hirschegg (Kleinwalsertal), Austria, July 16-19, 2006

2006/007 *Klimke, A.:* Efficient Construction of Hierarchical Polynomial Sparse Grid Interpolants using the Fast Discrete Cosine Transform

2006/008 *Buchukuri, T., Chkadua, O., Natroshvili, D.:* Mathematical modelling and analysis of interaction problems for metallic-piezoelectric composite structures with regard to thermal stresses

2006/009 *Merkle, C., Rohde, C.:* The Sharp-Interface Approach for Fluids with Phase Change: Riemann Problems and Ghost Fluid Techniques

2006/010 *Sändig, A.-M.:* Regularity results for linear elliptic boundary value problems in polygons. Lectures at the Charles University Prague, Oct.05

2006/011 *Flemisch, B., Kurz, S., Wohlmuth, B.:* A Framework for Maxwell's Equations in Non-Inertial Frames Based on Differential Forms

2006/012 *Sändig, A.-M.:* Nichtlineare Funktionalanalysis mit Anwendungen auf partielle Differentialgleichungen. Vorlesung im Sommersemester 2006

2006/013 *Rohde, C., Tiemann, N., Wen-An Yong:* Weak and Classical Solutions for a Model Problem in Radiation Hydrodynamics

2006/014 *Brunšen, S.:* Modeling and simulation of elastoplastic forming processes